AAV6-mediated Systemic shRNA Delivery Reverses Disease in a Mouse Model of Facioscapulohumeral Muscular Dystrophy

Sergia Bortolanza[1], Alessandro Nonis[2], Francesca Sanvito[3], Simona Maciotta[4], Giovanni Sitia[5], Jessica Wei[6], Yvan Torrente[4], Clelia Di Serio[2], Joel R Chamberlain[6] and Davide Gabellini[1]

[1]Dulbecco Telethon Institute and Division of Regenerative Medicine, San Raffaele Scientific Institute, Milano, Italy; [2]Università Vita-Salute San Raffaele, Milano, Italy; [3]Pathology Facility, San Raffaele Scientific Institute, Milano, Italy; [4]Department of Neurological Sciences, University of Milan, I.R.C.C.S. Foundation Ca' Granda, Ospedale Maggiore Policlinico, Milano, Italy; [5]Division of Immunology, San Raffaele Scientific Institute, Milano, Italy; [6]Division of Medical Genetics, Department of Medicine, University of Washington, Seattle, Washington, USA

Treatment of dominantly inherited muscle disorders remains a difficult task considering the need to eliminate the pathogenic gene product in a body-wide fashion. We show here that it is possible to reverse dominant muscle disease in a mouse model of facioscapulohumeral muscular dystrophy (FSHD). FSHD is a common form of muscular dystrophy associated with a complex cascade of epigenetic events following reduction in copy number of D4Z4 macrosatellite repeats located on chromosome 4q35. Several 4q35 genes have been examined for their role in disease, including *FRG1*. Overexpression of *FRG1* causes features related to FSHD in transgenic mice and the *FRG1* mouse is currently the only available mouse model of FSHD. Here we show that systemic delivery of RNA interference expression cassettes in the *FRG1* mouse, after the onset of disease, led to a dose-dependent long-term *FRG1* knockdown without signs of toxicity. Histological features including centrally nucleated fibers, fiber size reduction, fibrosis, adipocyte accumulation, and inflammation were all significantly improved. *FRG1* mRNA knockdown resulted in a dramatic restoration of muscle function. Through RNA interference (RNAi) expression cassette redesign, our method is amenable to targeting any pathogenic gene offering a viable option for long-term, body-wide treatment of dominant muscle disease in humans.

Received 3 May 2011; accepted 24 June 2011; published online 9 August 2011. doi:10.1038/mt.2011.153

INTRODUCTION

Facioscapulohumeral muscular dystrophy (FSHD) is the third most common human myopathy, with an incidence of 1 in 15,000 in the general population.[1] The disease is characterized by progressive degeneration of a highly selective set of muscle groups. As its name suggests, weakness first arises in facial mimic and shoulder girdle muscles. The disease can then progress to abdominal muscle leading to abdominal protrusion and spine lordosis. In more severe cases, muscle degeneration reaches foot dorsi-flexor and pelvic girdle muscles impairing the ability to walk. In addition to the muscular dystrophy, 50–75% of FSHD patients develop retinal vasculopathy highlighting the complex pathophysiology of FSHD.

FSHD has not been linked to a classical mutation within a protein-coding gene and several lines of evidence suggest that FSHD derives from the interplay of complex genetic and epigenetic events.[2] In 95% of cases (FSHD1A, OMIM 158900), the disease is associated with reduction in copy number within a large, complex tandem array, called D4Z4, located in the subtelomeric region of chromosome 4 (4q35).[3] While it is generally agreed that deletion of D4Z4 units causes epigenetic changes leading to the overexpression of genes present within the FSHD region, there are opposing opinions regarding support for a role for the D4Z4 repeat gene *DUX4*[4] and a proximal gene *FRG1*.[5] While efforts to produce a mouse model based on expression of *DUX4* have not succeeded, *FRG1*-expressing mice develop a disease with physiological, histological, ultrastructural, and molecular features of FSHD. *FRG1* is a highly conserved gene[6] encoding for a dynamic nuclear and sarcomeric protein.[7] In the nucleus, FRG1 is involved in RNA processing and colocalizes with proteins mutated in other neuromuscular disorders.[8–11] In mature muscles, FRG1 localizes also to the sarcomeric Z-disc.[7] Interestingly, in FSHD patients mild sarcomeric defects have been reported.[12] Notably, many other myopathies are caused by mutations in genes encoding for sarcomeric proteins.[13–15] Most importantly, overexpression studies in three different animal models indicate that *FRG1* is the only FSHD candidate gene able to recapitulate both muscular and vascular FSHD-like defects.[5,16–18] Collectively, these results suggest that the *FRG1* mouse is a valid model of FSHD.

There is no treatment for FSHD. The most straightforward therapeutic approach would be to eliminate the gene product that

The last two authors contributed equally to this work.

Correspondence: *Joel Chamberlain, Division of Medical Genetics, Department of Medicine, University of Washington, 1959 NE Pacific St., K-236B HSB, Seattle, WA 98195-7720, USA. E-mail: jrcham@uw.edu (or) Davide Gabellini, Division of Regenerative Medicine, San Raffaele Scientific Institute, DIBIT 2, 5A3-44 Via Olgettina 58, 20132, Milano, Italy. E-mail: gabellini.davide@hsr.it*

governs all pathogenic processes. We have developed a method, based on RNA interference (RNAi) to inhibit *FRG1*-mediated muscle pathology in the *FRG1* mouse model for restoration of muscle function. RNAi is a fundamental cellular mechanism for silencing gene expression[19] and is currently one of the most promising new approaches for disease therapy (reviewed in ref. 20).

For an efficient systemic delivery of RNAi to a difficult target tissue like the skeletal muscle, one promising strategy consists in the use of engineered viruses to express short hairpin RNAs (shRNAs).[21–23] Among the viral systems being utilized today, one that has generated much optimism is recombinant adeno-associated virus (rAAV) (reviewed in ref. 24). rAAVs possess several characteristics that make them interesting for gene therapy including absence of pathogenicity in humans, broad tissue tropism, and ability to infect postmitotic cells. Numerous AAV serotypes with preferential tropism for different tissues have been identified.[25–27] Intravenous administration of various rAAVs has proven successful at correction of disease in several animal models leading to a growing number of clinical trials to treat human disease such as hemophilia B, Parkinson's disease, and cystic fibrosis.[24] A single intravenous administration of rAAV serotype 6 (rAAV6) was shown to cause a body-wide transduction of the entire skeletal musculature[28] and was used for gene therapy studies of Duchenne muscular dystrophy in mice.[29] Recently, AAV6 delivery of therapeutic mini-dystrophin genes to larger animal models for long-term expression demonstrated success in preclinical studies.[30]

In contrast to gene replacement for disease therapy, we evaluated the feasibility of combining rAAV6 delivery and RNAi-mediated mRNA knockdown as a possible therapeutic approach for a dominant muscle disorder. We show that a single injection of rAAV6 expressing *FRG1* shRNAs into the tail vein of *FRG1* animals already showing signs of muscular dystrophy is safe and sufficient to obtain long-term *FRG1* knockdown. rAAV6 *FRG1* RNAi systemic application resulted in a significant histological, molecular, and functional rescue of the phenotype. This study opens a route to clinical application of single-dose, long-term RNAi therapy for the treatment of FSHD and other dominant muscular dystrophies.

RESULTS

Selection of a rAAV6-shRNA that efficiently downregulates *FRG1* expression

In order to efficiently downregulate the *FRG1* mRNA, we designed three different shRNAs (sh1-, sh2-, sh3-*FRG1*) (**Figure 1a**). The three shRNAs were cloned into a rAAV plasmid containing an RNAi expression cassette under the control of a human U6+27 snRNA promoter upstream of the a human placental alkaline phosphatase reporter gene (*hPLAP*) rAAV6-sh1*FRG1*, rAAV6-sh2*FRG1*, rAAV6-sh3*FRG1*) (**Figure 1a**).[31]

Viruses were initially tested for their ability to downregulate FRG1 in tissue culture by transducing C2C12 muscle cells overexpressing *FRG1*.[5] After 48 hours, *FRG1* messenger RNA levels were analyzed using real-time reverse transcriptase RT-PCR. As shown in **Figure 1b**, the *FRG1* downregulation achieved with rAAV6-sh1*FRG1* (0.52 ± 0.06, $P < 0.01$) was stronger compared to the one obtained with the other two viruses (0.67 ± 0.062 and 0.73 ± 0.08, for rAAV6sh2*FRG1* and rAAV6sh3*FRG1*, respectively). At protein level, a significant dowregulation following virus transduction was reached only with rAAV6-sh1*FRG1* (**Figure 1c**). Based on these data, we selected rAAV6-sh1*FRG1* for further tests *in vivo*.

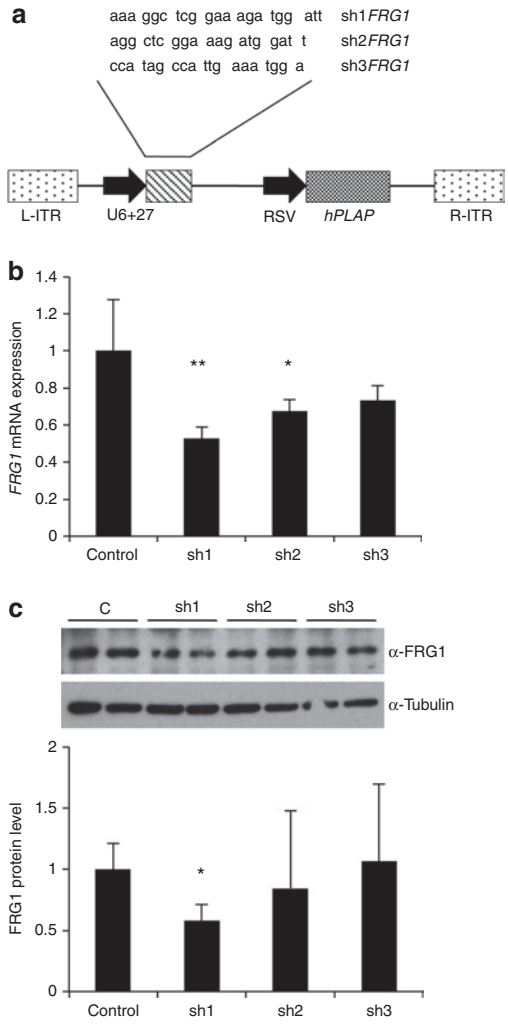

Figure 1 Design and *in vitro* efficacy of recombinant adeno-associated virus serotype 6 (rAAV6) driving expression of short hairpin RNAs (shRNAs) against *FRG1*. (**a**) Schematic representation of rAAV6 vector where shRNA sequences against *FRG1* (sh1, sh2, and sh3) are under the control of the U6 promoter. Rous Sarcoma Virus (RSV) promoter drives expression of human placental alkaline phosphatase (*hPLAP*). (**b**) Residual mRNA level of *FRG1* after infection of C2C12 myoblasts overexpressing *FRG1* with rAVV6 vector expressing sh1-, sh2- or sh3-*FRG1* sequences. The values were determined using real-time reverse transcriptase-PCR. (**c**) Residual protein level of FRG1 in the same sample as in panel **b**. A representative picture of the immunoblotting (top), and the quantification measured by densitometry (bottom) are shown. C, mock infected cells; sh1, rAAV6-sh1*FRG1* infected-cells; sh2, rAAV6-sh2*FRG1* infected-cells; sh3, rAAV6-sh3*FRG1* infected-cells. Error bars represents mean + SD, $n = 5$. $P < 0.05$ and $P < 0.01$ are represented by one or two asterisks, respectively.

Dose-dependent transduction of the entire skeletal musculature and long-term *FRG1* silencing

To evaluate the transduction potential of rAAV6-sh1*FRG1* after systemic delivery, *FRG1* mice were administered two different

doses of 2×10^{12} or 5×10^{12} vector genomes (vg), or vehicle as control, through the tail vein at 6 weeks of age. Importantly, at this age *FRG1* mice are already showing significant histological changes, such as reduction in muscle fiber cross-sectional area (CSA), increased percentage of centrally nucleated muscle fibers and inflammation (A. Xynos, M.V. Neguembor, M.C. Onorati, P. Picozzi, D. Licastro, S. Bortolanza *et al.*, in preparation). At 12 weeks postinjection, individual muscles were dissected and stained for the alkaline phosphatase reporter to determine the extent of transduction at the single muscle fiber level. As shown in **Figure 2**, all skeletal muscles analyzed confirmed the presence of the virus and displayed dose-dependent transduction. With the higher viral dose, all the muscles analyzed showed uniform transduction with greater than 80% positive muscle fibers. In contrast, with the lower dose the transduction was much less efficient and none of the muscles reached more than 45% of positively transduced muscle fibers (**Figure 2a,b**). Similar results were obtained by analyzing the level of mRNA of *hPLAP* by real-time RT-PCR in the different muscles. Indeed, the overall *hPLAP* expression level was between 6- (vastus lateralis) and 18- (tibialis anterior) fold higher at the higher viral dose as compared with the levels obtained in the same muscles injected with the lower viral dose (**Figure 2c**).

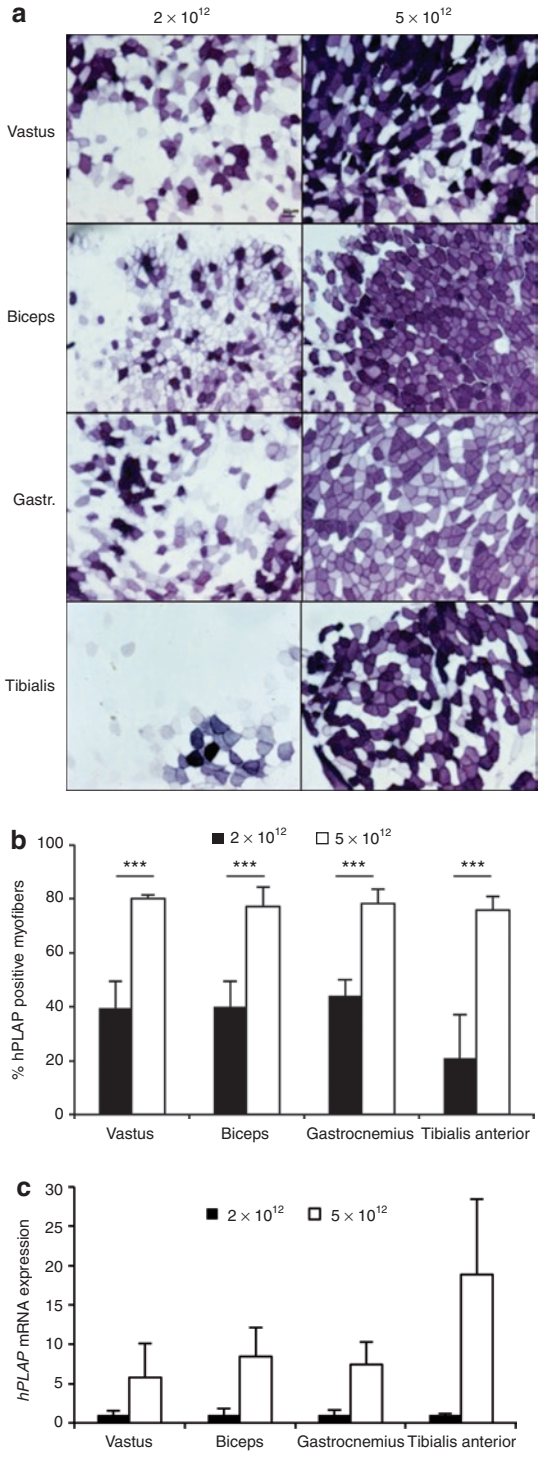

We next determined whether the transduction efficiency observed with the high dose of virus would translate into a higher level of *FRG1* muscle silencing. Using real-time RT-PCR, we found that the high viral dose of 5×10^{12} vg caused a significant reduction of *FRG1* expression in all muscles analyzed ($P < 0.01$ for vastus, $P < 0.05$ for other muscles) (**Figure 3a**). On the contrary, the viral dose of 2×10^{12} vg had no significant effect on mRNA levels of *FRG1*, indicating that the muscle transduction obtained was not sufficient to obtain a reproducible *FRG1* downregulation (**Figure 3a**).

In order to verify whether the downregulation observed at the RNA level with the high rAAV6-sh1*FRG1* dose translated into a downregulation at protein level, immunoblotting was performed to analyze FRG1 levels. We observed a reduction of FRG1 protein of 48–71% in the muscles analyzed as shown in **Figure 3b** and quantified in **Figure 3c**. Overall, our results indicate that a single rAAV6-sh1*FRG1* systemic administration is sufficient to transduce the entire skeletal musculature and obtain significant long-term *FRG1* silencing.

rAAV6-sh1*FRG1* treatment appears safe in mice

Although RNAi therapy in mice and humans appear to be generally effective and well tolerated, there are a number of reports from animal studies that caution against the use of high-dose *in vivo* as it can lead to oversaturation of the endogenous RNAi pathway.[32–35] Co-option of this pathway to suppress a specific disease gene could have adverse effects by interfering with the normal biological function of microRNAs (miRNAs) in targeted organs. Treatment

Figure 2 Transduction efficacy following systemic delivery of rAAV6-sh1*FRG1*. A total of 2×10^{12} or 5×10^{12} rAAV6-sh1*FRG1* viral genomes (vg) were administered by tail vein in 6-week-old *FRG1* overexpressing mice. Vastus lateralis, biceps brachii, gastrocnemius and tibialis anterior were harvested 12 weeks later. (**a**) Human placental alkaline phosphatase (hPLAP) activity in sections of skeletal muscles stained with the BCIP/NBT substrate. Representative images obtained using a ×10 objective are shown. (**b**) Quantification of hPLAP-positive myofibers in the indicated muscles. The percentage of hPLAP-stained myofibers versus total number of myofibers in the section is represented. Five fields for each muscle and three mice per group were analyzed. Values obtained from the mice injected with the dose of 2×10^{12} vg or 5×10^{12} vg are shown by black or white columns, respectively. Error bars represents mean + SD, $n = 3$ $P < 0.001$ is represented by three asterisks. (**c**) Real-time reverse transcriptase-PCR for *hPLAP* mRNA expression. The value obtained with the dose of 5×10^{12} vg (white bars) was related to the corresponding value obtained with the dose of 2×10^{12} vg (black bars) for each different muscle type.

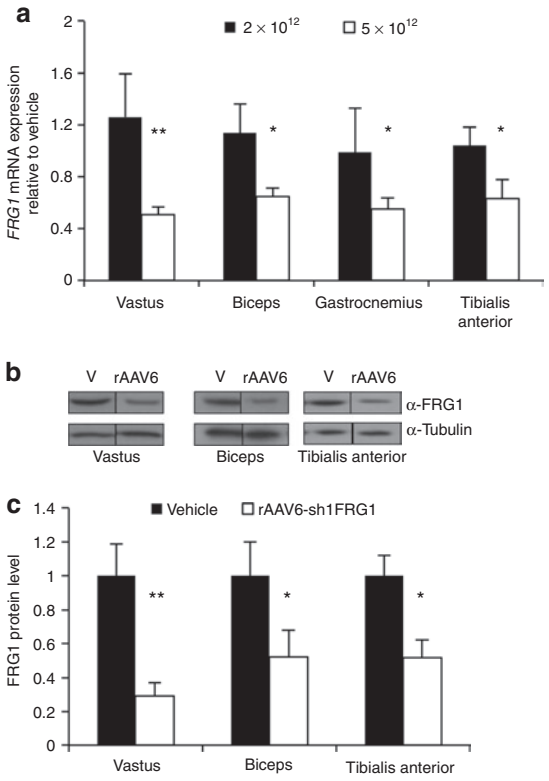

Figure 3 Efficient *FRG1* downregulation following systemic administration of rAAV6-sh1*FRG1*. (**a**) A total of 2 × 10^{12} vg or 5 × 10^{12} vg rAAV6-sh1*FRG1* were administered by tail vein in 6-week-old *FRG1* overexpressing mice. Vastus lateralis, biceps brachii, gastrocnemius and tibialis anterior were harvested 12 weeks later. Real-time reverse transcriptase-PCR for *FRG1* mRNA expression is represented. Values obtained from the mice injected with the dose of 2 × 10^{12} vg or 5 × 10^{12} vg are shown by black or white columns, respectively. Values were normalized versus vehicle-injected mice (n = 3). (**b**) Representative FRG1 and tubulin immunoblotting of muscles following systemic injection with 5 × 10^{12} vg. V, vehicle-injected; rAAV6, rAAV6-sh1*FRG1*-injected. (**c**) Immunoblotting quantification. Error bars represents mean + SD, n = 3. $P < 0.05$ and $P < 0.01$ are represented by one or two asterisks, respectively.

toxicity primarily correlated with shRNA dose and could be overcome by expressing extended hairpins such as miRNA-based hairpins that incorporated RNAi target sequences.[33,34] Therefore, achieving tissue tropism combined with efficacy-related shRNA expression levels, without overexpression, is important to minimize the risk of side effects from RNAi therapy. We combined a muscle-tropic AAV serotype, AAV6, with a human U6 expression cassette containing a 27 nucleotide 5′ leader for stabilization of the transcript and a 3′ poly(U) terminator.[31] In this setting we did not observe any adverse events related to treatment with *FRG1*-targeted hairpins. Safety of rAAV6-sh1*FRG1* was evaluated at multiple levels and time points after systemic delivery. As previously reported[28] and shown in **Supplementary Figure S1a**, liver and the heart are two vital organs efficiently transduced by AAV6. We collected blood samples 1, 4, and 8 weeks after the injection to measure the serum activity of alanine transaminase levels for an indication of liver toxicity. **Supplementary Figure S1b** shows that rAAV6-sh1*FRG1* transduced mice displayed comparable serum alanine aminotransferase activity to saline injected or wild-type mice at all timepoints, including 4 weeks postinjection, the peak of liver toxicity observed by others assaying AAV-mediated RNAi cassette expression in liver.[32] Histological analysis showed that livers of treated mice were indistinguishable from those of untreated animals indicating an absence of ongoing liver toxicity of rAAV6-sh1*FRG1* (**Supplementary Figure S1c**). We also looked for loss of cardiomyocytes, since cardiomyocyte death in the ventricular wall and associated dilated cardiomyopathy results from inhibition of the miRNA pathway necessary for normal heart function.[36] As shown in **Supplementary Figure S1c**, histological analysis of rAAV6-sh1*FRG1* transduced hearts did not showed any signs of toxicity as no lesions were detected. Furthermore, we considered the potential for unintended changes in skeletal muscle caused by the therapy. As a measure of fiber integrity, we analyzed expression and distribution of dystrophin that is normally positioned at the membrane of muscle fibers. As shown in **Supplementary Figure S2a**, integrity of the sarcolemma was unaffected by rAAV6 treatment as demonstrated by normal localization of dystrophin. Next, we measured expression of the inflammatory cytokines, interleukin-10 and tumor necrosis factor-α (**Supplementary Figure S2b**). rAAV6-sh1*FRG1* treated animals displayed a level of inflammation reduced compared to vehicle-treated *FRG1* animals. Additionally, in order to exclude that rAAV6-mediated sh1*FRG1* expression interfered with miRNA production pathways, we analyzed the levels of miRNA expression in different tissues. As shown in **Supplementary Figure S2c**, the expression of the miRNAs analyzed was comparable in vehicle and rAAV6-sh1*FRG1* treated *FRG1* mice. Altogether, our analyses indicate that long-term rAAV6-sh1*FRG1* treatment is safe.

A single intravenous injection of rAAV6-sh1*FRG1* rescues muscle histopathology of *FRG1* mice

Based on our observation that a single systemic administration of 5 × 10^{12} vg of rAAV6-sh1*FRG1* is safe and is sufficient to obtain high transduction levels and significant long-term downregulation of *FRG1* expression in all muscles analyzed, we proceeded to evaluate long-term therapeutic efficiency of rAAV6-sh1*FRG1*. We administered virus at 6 weeks of age, past the onset of dystrophic muscle changes (A. Xynos, M.V. Neguembor, M.C. Onorati, P. Picozzi, D. Licastro, S. Bortolanza *et al.*, in preparation). Animals were analyzed 3 months postinjection of a single dose of 5 × 10^{12} vg. We focused our analysis on vastus lateralis, a muscle highly affected in *FRG1* mice and in FSHD patients.[5] Histological examination of Gömöri trichrome stained muscle sections revealed a general qualitative improvement in fiber size and muscle architecture (**Figure 4a**). Analysis of several muscular dystrophy parameters revealed a significant quantitative rescue. First, there was a 30% reduction ($P < 0.001$) in centrally nucleated myofibers in the vastus muscle of rAAV6-sh1*FRG1* treated animals, indicating an inhibition of muscle degeneration and regeneration processes (**Figure 4b**). Second, morphometric analysis to determine the individual muscle fiber CSA showed that the distribution of CSA in rAAV6-sh1*FRG1* treated mice was significantly different than the vehicle-treated mice (Kolmogorov–Smirnov test) (**Figure 4c**). The CSA distribution curve was shifted right or toward larger overall fiber area for the rAAV6-sh1*FRG1* treated animals compared to vehicle-injected

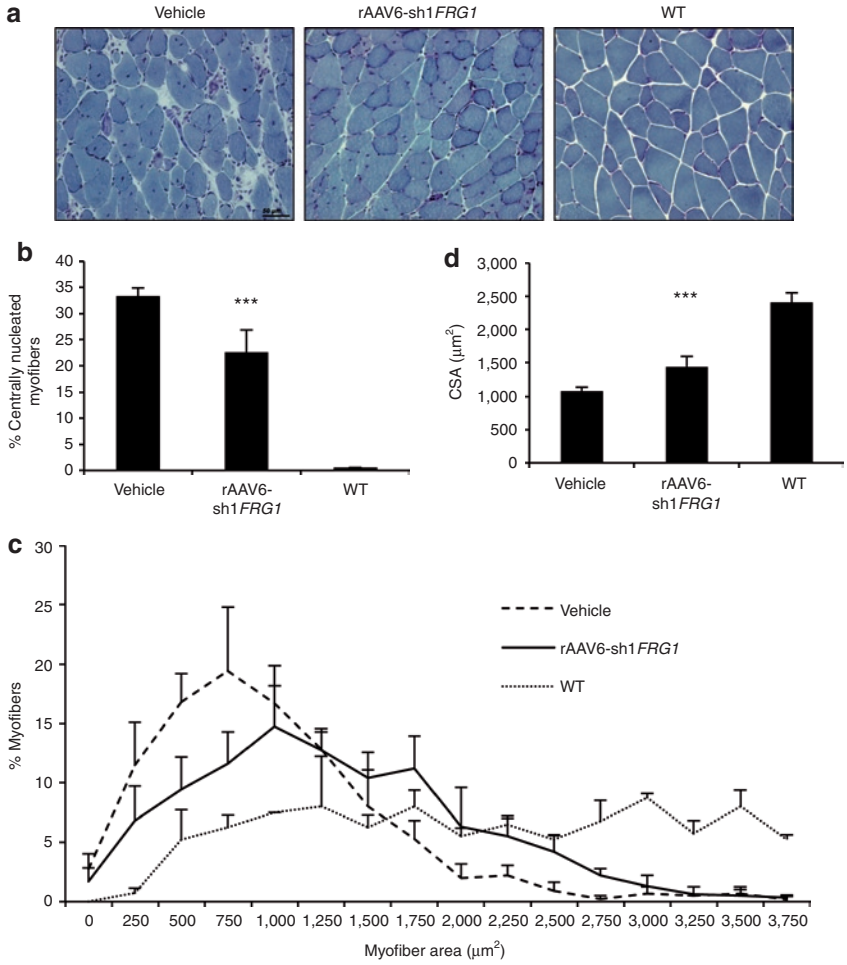

Figure 4 Significant rescue of muscle morphology after a single injection with rAAV6-sh1*FRG1*. 5×10^{12} vg of rAAV6-sh1*FRG1* were administered in the tail vein in 6-week-old *FRG1* overexpressing mice. Twelve weeks after the injection, the vastus lateralis were analyzed by Gömöri trichrome staining. Vehicle-injected *FRG1* mice and age-matched wild-type (WT) mice were used as control. (**a**) Representative vastus lateralis sections obtained using a ×20 objective. Bar = 50 μm; (**b**) Centrally nucleated fibers were counted in vastus lateralis of the different mice groups and represented as percentage of total myofibers; (**c**) Cross-sectional area (CSA) was measured in vastus lateralis and the average of each group is represented; (**d**) Distribution of fiber area. Error bars represents mean + SD, $n = 5$ per vehicle- and rAAV6-sh1*FRG1*-injected mice, $n = 3$ per age-matched WT mice. $P < 0.001$ is represented by three asterisks.

controls. The increase in muscle fiber CSA of the treated mice was more similar to that of age-matched wild-type control animals (**Figure 4c**). This result is also supported by the average CSA of rAAV6-sh1*FRG1* treated animals, which was increased by 30% ($P < 0.001$) compared to that of vehicle-treated control mice (**Figure 4d**). Third, we evaluated fibrosis in the treated mice, a common characteristic of dystrophic muscle. Sirius red staining for fibrosis-associated collagen deposition indicated that treated muscles displayed a 35% ($P < 0.001$) less collagen protein than controls (**Supplementary Figure S3**). Fourth, Oil Red O staining showed more than 50% ($P < 0.01$) less adipose tissue than in saline-treated mice (**Supplementary Figure S4**), a replacement for loss of muscle tissue commonly associated with dystrophic muscle changes. Finally, immunohistochemistry staining against CD45, a surface marker for all cells of hemopoietic origin, showed a 44% ($P < 0.001$) decrease of the inflammatory infiltrates in treated animals, consistent with the reduction in inflammatory cytokines shown in **Supplementary Figure S2** (**Supplementary Figure S5**). Collectively, these results show that a single systemic delivery of rAAV6-sh1*FRG1* is sufficient to obtain a significant rescue in muscle histopathology of *FRG1* mice.

rAAV6-sh1*FRG1* rescues muscle function

Our results show that rAAV6-sh1*FRG1* can mediate long-term *FRG1* downregulation that results in an amelioration of muscle histopathology. Therefore, we wanted to determine whether the improvement in histopathology observed also reflected improvement in muscle function. For this purpose, we decided to perform exercise tolerance tests. Animals injected with rAAV6-sh1*FRG1*, vehicle-treated animals or wild-type mice underwent a treadmill running test during the 11-week post-transduction period and were monitored for the length of time necessary to reach exhaustion. As shown in **Figure 5** and in the online video (**Supplementary Video S1**), rAAV6-sh1*FRG1*-treated animals showed an improvement in performance as early as 5 weeks after treatment and by the end of the 11-week test period their performance was indistinguishable

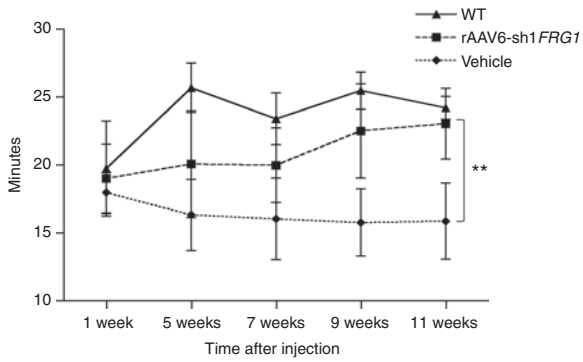

Figure 5 Increased muscles function following single intravenous administration of rAAV6-sh1*FRG1* vector. 5×10^{12} vg of rAAV6-sh1*FRG1* were injected in the tail vein of *FRG1* overexpressing mice. Treadmill running exercise was performed during 11 weeks after treatment and the time (minutes) to reach exhaustion was recorded. Vehicle-injected mice and C57BL/6J mice were used as controls. Error bars represents mean + SD, $n = 5$ per vehicle- and rAAV6-sh1*FRG1*-injected mice, $n = 4$ per age-matched wild-type (WT) mice. $P < 0.01$ is represented by two asterisk and it represents the statistical difference between vehicle and vector-injected mice at 9 and 11 weeks after treatment.

from wild-type animals, indicating that their functional recovery was complete. In contrast, vehicle-treated mice, in which disease progression continued, did not display any improvement in running capability throughout the test (**Figure 5**).

Reversal of disease is specific to FRG1 downregulation

Our analyses of rAAV6-sh3*FRG1* did not show any significant knockdown activity of *FRG1* mRNA or protein with widespread transduction of muscle (**Figure 1**), so we decided to test this viral preparation further in *FRG1* mice to rule out the possibility of RNAi nonspecific effects of rAAV6-sh1*FRG1* treatment. As shown in **Figure 6**, injection of 5×10^{12} vg of rAAV6-sh3*FRG1* was very effective in transducing several muscles but did not cause any *FRG1* downregulation. Interestingly, we also did not observe any histological or functional phenotypic rescue in *FRG1* mice with rAAV6-sh3*FRG1* treatment (**Figure 6**). These results indicate that the phenotypic rescue is specifically due to *FRG1* knockdown.

DISCUSSION

Muscular dystrophies pose a major public health problem since they are common, incurable disorders that result in significant disability or death. Historically, FSHD was thought of as the third most prevalent muscular dystrophy. Notably, new epidemiological data suggest that FSHD could be the most prevalent muscular dystrophy followed by Duchenne/Becker and myotonic dystrophies: http://www.orpha.net/consor/cgi-bin/Education_Home.php?lng=EN. So far, development of therapeutic approaches for muscular dystrophies has been mainly focused on Duchenne muscular dystrophy. Understanding the complex mechanism of disease development for FSHD has slowed therapy development and, until the work we describe here, there was little prospect for a treatment for FSHD.

It is generally agreed that FSHD results from gene overexpression.[2] For this reason, FSHD provides an ideal opportunity to explore the therapeutic potentials of RNAi-mediated gene silencing. Since FSHD is caused by a single event (gene overexpression following D4Z4 deletion), our RNAi therapeutic approach would be applicable to all patients. Moreover, FSHD has a delayed onset, and through molecular genetic testing, individuals carrying the molecular defect can be identified long before they present clinical signs of muscular dystrophy. Hence, there is a considerable therapeutic window where intervention may slow or even prevent disease-related muscle deterioration.

Although several intriguing FSHD candidates have been proposed, no single gene has been conclusively linked to FSHD development thus far.[3] It was reported that the D4Z4 repeat contains an ORF encoding a double homeobox protein named DUX4.[37] DUX4 has been detected in FSHD-derived primary myoblasts but not in controls, suggesting that D4Z4 may directly affect disease progression through the aberrant production of DUX4.[4,38-40] Several functional studies described extreme general toxicity for DUX4.[41–44] Cellular toxicity of DUX4 coupled with very low DUX4 expression in human cells poses a difficult challenge for modeling the human disease in mice. However, if a *DUX4* mouse model is produced, our approach could be adapted for *DUX4* knockdown in muscle through retargeting of the RNAi hairpin sequence to *DUX4* mRNA.

A growing understanding of its function, strongly suggests that *FRG1* overexpression plays an important role in FSHD.[16–18,45] Based on these data, *FRG1* inhibition would be expected to lead to a therapeutic benefit in FSHD. Hence, we have used the only available FSHD mouse model to provide a proof of principle with respect to the use of RNAi therapeutic approaches for FSHD. In this study, we demonstrated long-term, dose-dependent reduction in *FRG1* expression in all the muscles analyzed. Therapeutic benefits were observed in all of the mice treated with either low or high AAV6-sh1*FRG1* doses. However, only the high-dose cohorts had therapeutic levels of *FRG1* knockdown that were sufficient and sustainable to obtain a near complete functional recovery. The low-dose cohorts were on the threshold of a moderate to severe muscle histology phenotype that correlated with clinical observations of a variable and minor functional recovery (data not shown). Interestingly, we observed variability in skeletal muscle gene transfer efficacy in rAAV6 shRNA-injected *FRG1* mice injected with lower vector dose (**Figure 2** and data not shown) suggesting that it was just at the threshold level.

An indication that viral-based RNAi expression cassette expression could cause toxicity in mice due to oversaturation of the endogenous miRNA pathways came from a study of AAV-mediated shRNA hairpin expression in liver by Grimm and colleagues.[32] Toxicity was also reported in the context of targeting mutant Huntington's disease mRNA.[34] In both cases, toxicity was determined to be a function of shRNA processing and expression level. Interestingly, Davidson's group reported that toxicity was eliminated when RNAi hairpin sequences were incorporated into a naturally occurring miRNA scaffold.[34] We selected a version of the U6 promoter to achieve levels of expression that might be therapeutic in the context of systemic delivery and high transgene expresssion. The U6+27 expression cassette had been developed for stable nuclear expression and 5′ capping of small RNAs, such as ribozymes, to direct cleavage of potential therapeutic targets as demonstrated for the TAR sequence from HIV-1 and was adapted for expression of hairpin triggers of RNAi.[31] Notably, using the

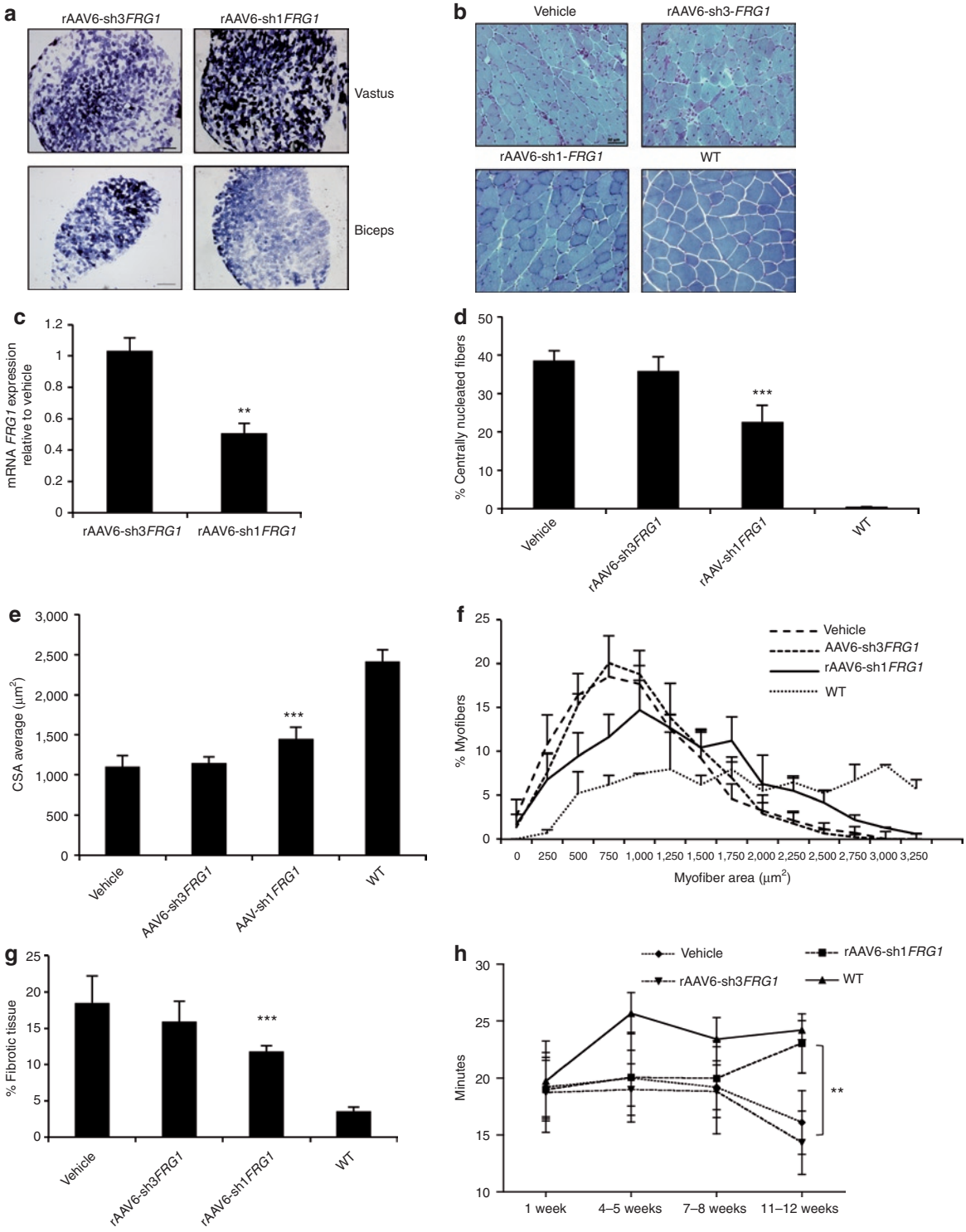

Figure 6 Phenotypic rescue is specifically due to *FRG1* knockdown. 5×10^{12} vg of the non-silencing rAAV6-sh3*FRG1* or rAAV6-sh1*FRG1* were injected in the tail vein of *FRG1* overexpressing mice. Animals were analyzed 12 weeks later. (**a**) Human placental alkaline phosphatase (hPLAP) activity in section of skeletal muscles stained with the BCIP/NBT substrate. Bar = 100 µm. (**b**) Representative images of vastus lateralis Gömöri trichrome staining in vehicle-, rAAV6-sh1*FRG1*- or rAAV6-sh3*FRG1*-injected *FRG1* mice and age-matched wild-type (WT) mice obtained using a ×20 objective. (**c**) Real-time reverse transcriptase-PCR for *FRG1* mRNA expression. Values were normalized versus vehicle-injected mice. (**d**) Centrally nucleated fibers were counted in vastus lateralis of different mice group and represented as percentage of total myofibers. (**e**) Cross-sectional area (CSA) was measured in vastus lateralis and the average of each group is represented. (**f**) Distribution of muscle fiber area. (**g**) Area occupied by fibrotic tissue was quantified and expressed as percentage of total muscle area. (**h**) Treadmill running exercise was performed during 12 weeks of treatment and the time (minutes) to reach exhaustion was taken. The statistical analysis is refereed to rAAV6-sh1*FRG1*- versus rAAV6-sh3FRG1-injected mice at the last time point of the assay. $N = 4$ per vehicle, $n = 5$ per rAAV6-sh3*FRG1*- and rAAV6-sh1*FRG1*-injected mice and age-matched WT mice. $P < 0.01$ is represented by two asterisks; $P < 0.001$ is represented by three asterisks.

U6+27 promoter for expression of HIV and lamin A/C RNAi hairpin triggers led to efficient suppression of target genes in human cells and did not show accumulation of full-length precursors.[46] It is unclear from the small number of RNAi sequences tested whether the U6+27 expression cassette will have a safety profile *in vivo* similar to recent tests of miRNA-based RNAi shuttles or RNA polymerase II promoter expression cassettes and needs to be examined further.[33,34] Nevertheless, no long-term evidence of toxicity was observed in any of the treated mice using the U6+27 promoter to express our therapeutic hairpins.

In conclusion, we have shown that we can prevent disease progression with systemic, AAV6-mediated *FRG1* RNAi performed following disease onset. This work exemplifies the power and specificity of RNAi in a widespread tissue in a living animal and offers a potential route to clinical application and treatment for individuals who are already showing symptoms of disease. The efficient, stable, long-term therapeutic reduction of pathological signs in the *FRG1* mouse suggests the added potential clinical benefit of efficacy with limited dosing. This therapy allowed significant improvement of disease and could potentially be translated to human patients. The knowledge gained through these studies could facilitate the development of new therapies to treat FSHD and other dominant diseases.

MATERIALS AND METHODS

RNAi hairpin design and cloning. The original RNAi *FRG1* targets were select using a program previously available on the Promega website based on parameters specified in the scientific literature (siRNA Designer, contact Promega, Madison, WI for details). Three *FRG1* siRNAs were tested *in vitro* and two were selected for their knockdown efficiency of exogenously expressed FRG1 as analyzed by western blot (data not shown). From the first target sequence from *FRG1* exon 8 shown in **Figure 1**, the full-length (*FRG1*sh1) and a shortened sequence by 2 nts from the 5′ end (*FRG1*sh2) to increase safety *in vivo*[32] were cloned as hairpins using the overlapping oligonucleotides: sh1 = full-length 5′ ACGCGTCGAC AAAGGCTCGGAAAGATGGATTCTTCCTGTCAAA 3′ and 5′ TGCTC TAGAAAAGGCTCGGAAAGATGGATTTGACAGGAAGAA 3′; sh2 = 5′ ACGCGTCGACAGGCTCGGAAAGATGGATTCTTCCTGTCAAA 3′ and 5′ TGCTCTAGAAGGCTCGGAAAGATGGATTTGACAGGAAG AA 3′. Oligonucleotides designed from the second selected siRNA from exon 3 to make *FRG1*sh3 are as follows: 5′ ACGCGTCGACCCATAGCC ATTGAAATGGACTTCCTGTCATC 3′ and 5′ TGCTCTAGACCATAGC CATTGAAATGGATGACAGGAAGTC 3′. These oligonucleotide pairs were annealed, extended, then restricted with *Sal* I and *Xba* I and cloned into the *Sal* I and *Xba* I sites of the U6+27 expression cassette cloned into pARAP4. The full cassette, U6+27-Sal I/Xba I-TTTTT, was derived from lentiviral plasmid pLGINm and inserted into pARAP4 (existing *Sal* I and *Xba* I sites destroyed)[47] by blunt-end cloning of *Cla* I and *EcoR* I restricted fragment into the *SnaB* I site 5′ of the RSV-*hPLAP* gene (kind gift from Chao-Zhong Song, University of Washington, Seattle, WA) described in ref. 48.

Virus production. AAV6 production was essentially as described in ref. 28 with modification described in ref. 49. Viral genomes were quantitated by Southern analysis using a probe to the *hPLAP* SV40 polyadenylation signal as described in ref. 50.

Manipulation of experimental animals. C57BL/6J transgenic mice overexpressing human *FRG1* under the control of the human skeletal α-actin gene promoter[5] were maintained by crossing them with wild-type C57BL/6J mice. *FRG1*-high mice and control C57BL/6J littermates were maintained at Charles River (Calco, Italy). All procedures were approved by the Institutional Animal Care and Use Committee of the Fondazione San Raffaele del Monte Tabor and were communicated to the Ministry of Health and local authorities according to Italian law.

Mice progeny were genotyped by PCR using the primers 5′-GA TCTAGCGGCCGCCATGGCCGAGTACTCCTATGTGAAGTCT-3′ and 5′-GCGCGCTTAATTAATCACTTGCAGTATCTGTCGGCTTTCA. PCR conditions were as follows: initial denaturation at 95 °C for 2 minutes, 42 cycles with denaturation at 95 °C for 30 seconds, annealing at 68 °C for 30 seconds and amplification at 72 °C for 1 minute. Virus was administered by intravenous injection via tail vein to 6-weeks-old transgenic female mice. In detail, 200 µl containing 2×10^{12} or 5×10^{12} vg of vector in physiological solution were injected into the tail vein using a 25-gauge Terumo syringe (Terumo, Leuven, Belgium). Mice injected with an equal volume of physiological solution (vehicle) and wild-type sex and age-matched C57BL/6J were used as controls. All mice were evaluated during 12 weeks subsequent to treatment.

Cell culture and viral infection. *FRG1* overexpressing C2C12 myoblast cells were previously described.[5] Cells were grown in DMEM-HIGH (Dulbecco's modified Eagle's medium, high glucose with sodium pyruvate and L-glutamine; EuroClone, Milano, Italy) supplemented with 10% fetal bovine serum (EuroClone), 1% penicillin/streptomycin (100 U/ml final concentration; EuroClone) and 1 µg/µl Neomycin (G-418; InvivoGen, San Diego, CA). All cells were maintained at 37 °C with 5% CO_2 in a humidifier incubator.

Cells were seeded in 6-well plates with 1×10^4 cells/well and were infected 24 hours later with 10^{10} vg/well of rAAV6 expressing sh1, sh2, and sh3. After 3 days, cells were collected for RNA and protein analysis.

Histological analysis. Mice were euthanized by CO_2 inhalation or by cervical dislocation. Skeletal muscle tissue specimens were rapidly mounted in OCT (Optimal Cutting Temperature compound; Sakura, Zoeterwoude, The Netherlands) and then frozen in isopentane cooled in liquid nitrogen. Transverse sections (8 µm) were performed on a cryostat and used for the analysis described below.

The percentage of centrally nucleated fibers and the CSA of single muscle fibers were determinate by using ImageJ software (NIH, Bethesda, MD) on calibrated images of cryosections stained with Gömöri Trichrome.

Characterization of fibrotic and fat tissue in the muscle was performed after Sirius Red and Oil Red O staining, respectively. The tissues were quantified measuring the percentage of red area in the sections (ImageJ, NIH).

For CD45 immunohistochemistry, cryostat sections were air-dried and fixed in prechilled acetone for 10 minutes. Endogenous peroxidase was inhibited by incubation for 10 minutes at room temperature with methanol plus 0.03% hydrogen peroxide. Tissue sections were incubated overnight at 4 °C with rat, anti-mouse CD45 antibody (BD, Franklin Lakes, NJ) diluted 1:500. Then samples were incubated with 1:300 dilution of an anti-rat antibody conjugated with biotin (#13-4813-85; eBioscience, San Diego, CA). Avidin-biotin-peroxidase complex was added (Vector lab, Burlingame, CA) and sections were incubated for 5–10 minutes with a DAB substrate (Dako, Glostrup, Denmark) and counterstained with hematoxylin and mounted.

For dystrophin immunofluorescence, cryostat sections were permeabilized with 0.2% TritonX100 and 1% bovine serum albumin for 15 minutes. After a blocking of 30 minutes in 0.2% TritonX100, 1% bovine serum albumin and 10% goat serum, the sections were incubated O/N with a mix of two anti-mouse Dystrophin antibodies (NCL-Dys1 and NCL-Dys2; Novacastra, Leica Microsystem, Wetzlar, Germany) diluted 1:50. Then samples were incubated for 1 hour with 1:500 dilution of a goat anti-mouse Alexa Fluor 555 (Invitrogen, Cergy-Pontoise, France). Finally, nuclei were stained by Hoechst3342 and section were mounted in phosphate-buffered saline 90% glycerol.

For the analysis of human alkaline phosphatase (hPLAP) activity, muscles cryosections were fixed in 4% paraformaldehyde for 10 minutes, incubated at 65 °C for 90 minutes to inactivate endogenous APs and stained at room temperature protected from the light with BCIP/NBT substrate (Roche, Basel, Switzerland) in a buffer containing 100 mmol/l Tris-HCl pH 9, 150 mmol/l NaCl, 1 mmol/l $MgCl_2$, 0.001% Tween20. Next, sections were dehydrated in an alcohol scale and mounted.

Following euthanization, mouse livers and heart specimens were collected and paraffin embedded. Sections of 8 µm were cut and stained with hematoxylin and eosin.

RNA isolation and real-time RT-PCR. Total RNA was extracted from cells with PureLink RNA MiniKit (Invitrogen, Carlsbad, CA) following the manufacturer's instructions. Dissected muscles were disrupted by TissueLyser (Qiagen, Hilden, Germany) and RNA was isolated using RNeasy fibrous tissue kit (Qiagen).

Equal amounts of RNA for each sample were retrotranscribed with SuperScript III First-Strand Synthesis SuperMix (Invitrogen, Carlsbad, CA) following the manufacturer's conditions. In brief, RNA was retrotranscribed with a 1:1 mix of oligo(dT) and random hexamer primers and with SuperScript III Reverse Transcriptase (Invitrogen, Carlsbad, CA). After treatment, the complementary DNAs were digested with RNaseH for 20 minutes at 37 °C.

For gene expression analysis, real-time PCR with Sybr GreenER qPCR kit (Invitrogen, Carlsbad, CA) was used. Each sample was run in triplicate with specific primers for *FRG1* (forward 5′-AGTCCTCCAGAGCAGTTTAC-3′, reverse 5′-AATAAAGCAGCTATTTGAGGC-3′) and *hPLAP* (forward 5′-GGTGAACCGCAACTGGTACT-3′, reverse 5′-CCCACCTTGGCTGTAGTCAT-3′). *IL-10* (forward 5′-ATTTG-AATTCCCTGGGTGAGAAG-3′, reverse 5′-CACAGGGGAGAAATCGATGACA-3′) and *TNF-α* (forward 5′-TCCCAGGTTCTCTTCAAGGGA-3′, reverse 5′-GGTGAGGAGCACGTAGTCGG-3′).

For sample normalization, *GAPDH* (forward 5′-TCAAGAAGGTGGTGAAGCAGG-3′, reverse 5′-ACCAGGAAATGAGCTTGACAAA-3′) or *ACTN3* (forward 5′-GGGGCGGCGAGTACATGGAAC-3′, reverse 5′-CAGTGAAGGTTTTCCGCTGCTGT-3′) were used in cell or muscle samples, respectively. The PCR conditions were the following: initial denaturation at 95 °C for 10 minutes, 40 cycles with denaturation at 95 °C for 30 seconds, annealing at 58 °C for 30 seconds and amplification at 72 °C for 30 seconds.

Gene expression of *IL-10* (forward 5′-ATTTG-AATTCCCTGGGTGAGAAG-3′, reverse 5′-CACAGGGGAGAAATCGATGACA-3′) and *TNF-α* (forward 5′-TCCCAGGTTCTCTTCAAGGGA-3′, reverse 5′-GGTGAGGAGCACGTAGTCGG-3′) was normalized versus *GAPDH* and the conditions of the PCR were the following: 50 °C for 2 minutes, 95 °C for 10 minutes, 40 cycles with 95 °C for 15 seconds and 60 °C for 1 minute. Melting curves were performed at the end of each amplification reaction to monitor product specificity.

Viral genome quantification. Vector genomes per nuclei from injected mice were determined by real-time qPCR on an ABI Prism 7500 (Perkin Elmer, Waltham, MA) with primers to the SV40 polyadenylation signal [forward- 5′ TTTTCACTGCATTCTAGTTGTGGTT 3′ and reverse- 5′ CATGCTCTAGTCGAGGTCGAGAT 3′ with probe 5′ 6FAM-ACTCATCAATGTATCTTATCATG-MGBNFQ 3′ (Applied Biosystems, Austin, TX)]. Nuclear mouse *Ldlr* was quantified [forward primer- 5′ CGTGCTCCCAGGATGACTTC 3′ and reverse primer 5′ CTCCATCACACACAAACTGCG 3′ and detected with probe- 5′ 6FAM-ATGCCAGGATGGCAAGTGCATCTCC-TAMRA (Operon, Huntsville, AL)] and used to determine the vector genomes per nuclei (vg/n) based on the number of genomes/(number of copies of *Ldlr*/2).

Western blotting. Cells or dissected muscles were homogenized in RIPA buffer (50 mmol/l Tris pH = 7.4, 150 mmol/l NaCl, 1% Triton X100, 1% deoxycholic acid, 0.1% sodium dodecyl sulfate) supplemented with a cocktail of protease inhibitors (Complete Tablets; Roche, Basel, Switzerland) using a TissueLyser (Qiagen). Samples were incubated for 30 minutes on ice and centrifuged at 16,500*g* for 10 minutes at 4 °C. The supernatant was removed and centrifuged again. Protein concentration of the final supernatant was measured using the Bradford assay (Pierce, Rockford, IL). Ten micrograms of protein extracts were separated using a 10% sodium dodecyl sulfate-polyacrylamide gel electrophoresis gel and transferred onto a nitrocellulose membrane (GE Healthcare, Buckinghamshire, UK). Immunoblots were incubated with primary antibodies against either human FRG1 (mouse monoclonal, 1:500, sc-101050; Santa Cruz, San Diego, CA) or HA (mouse monoclonal, 1:500 #MMS-101; Covance, Princeton, NJ). Subsequently, 1:10,000 dilution peroxidase-conjugated donkey anti-mouse IgG (#715-035-015; Jackson ImmunoResearch, West Grove, PA) was added. Detection was performed by super signal west pico chemioluminescence substrate (Thermo Scientific, Waltham, MA). Homogeneous sample loading was verified with an anti-α tubulin antibody (T9026; Sigma, St Louis, MO) at 1:10,000 dilution.

Blood analysis. The extent of hepatocellular injury was monitored by measuring serum alanine aminotransferase activity at multiple time points after AAV injection. Serum alanine aminotransferase activity was measured with a IFCC (International Federation of Clinical Chemistry and Laboratory Medicine) optimized kinetic UV method in a SABA chemical analyzer (SEAC-RADIM, Firenze, Italy) and expressed as U/L (Units/Liter).

Functional analysis. Three groups of mice (wild type $n = 4$ age- and sex-matched, transgenic *FRG1* vector-injected $n = 5$, transgenic *FRG1* vehicle-injected $n = 5$) were subjected to an exhaustion treadmill test from 1 to 12 weeks after treatment. Each mouse was placed on the belt of a six-lane motorized treadmill (Exer 3/6 Treadmill; Columbus Instruments, Columbus, OH) supplied with shocker plates. The treadmill was run at an inclination of 0° initially at 4 m/minute for 2 minutes and the speed was then increased 2 m/minute every 2 minutes at an inclination of 0°. The test was stopped when the mouse remained on the shocker plate for more than 20 seconds without attempting to re-engage the treadmill, and the time to exhaustion was determined.

miRNA extraction and quantitative RT-PCR analyses. Small RNAs were isolated from the heart, liver and skeletal muscles of *FRG1* overexpressing mice infected with AVV6-sh1*FRG1* ($n = 3$) or vehicle alone ($n = 3$) using miRNeasy FFPE kit (liver and heart) (Qiagen) or miRNeasy mini kit (skeletal muscles) (Qiagen). For miRNA detection, RNA was retrotranscribed and quantified by qPCR using the TaqMan MicroRNAs assay (Applied Biosystems). SnoRNA55 was used to normalize the expression and quantitative PCR was performed on a ViiA7 (Applied Biosystems).

Statistical analysis. All data are expressed as means ± SD. Difference between two groups was tested by means of two-tail *t*-test for independent samples. A Kolmogorov–Smirnov test was performed to determine whether the fiber distribution was similar in different samples.

SUPPLEMENTARY MATERIAL

Figure S1. Absence of toxicity in liver and heart of rAAV6-sh1*FRG1* treated mice.

Figure S2. Absence of toxicity in muscle and normal miRNA expression following rAAV6-sh1*FRG1* treatment.

Figure S3. rAAV6-sh1*FRG1* reduces fibrosis in *FRG1* overexpressing mice muscles.

Figure S4. rAAV6-sh1*FRG1* reduces fat deposition in *FRG1* overexpressing mice muscles.

Figure S5. rAAV6-sh1*FRG1* reduces inflammation in *FRG1* overexpressing mice muscles.

Video S1. Treated FRG1 mice show improved running endurance.

ACKNOWLEDGMENTS

We thank Jeffrey Chamberlain, James Allen, and Eric Finn for assistance with virus preparation and Choa-Zhong Song and George Stamatoyannopoulos for providing the U6 expression cassette used in these studies. Support for the JR Chamberlain laboratory came from the Pacific Northwest Friends of FSH Research and the Muscular Dystrophy Association USA (MDA). Research in the Gabellini laboratory is made possible by support provided by the European Research Council (ERC), the Italian Ministry of Health, MDA USA, the Association Française contre les Myopathies (AFM), the FSHD Global Research Foundation, a Jaya Motta private donation and the FSH Society, Inc. D.G. is a Dulbecco Telethon Institute Assistant Scientist.

REFERENCES

1. Flanigan, KM (2004). Facioscapulohumeral muscular dystrophy and scapulo-peroneal disorders. In: Engel, A, Franzini-Armstrong, C (eds). *Myology*, 3th edn., vol. 2. McGraw Hill: New York. pp 1123–1133.
2. Neguembor, MV and Gabellini, D (2010). In junk we trust: repetitive DNA, epigenetic and facioscapulohumeral muscular dystrophy. *Epigenomics* **2**: 271–287.
3. Cabianca, DS and Gabellini, D (2010). The cell biology of disease: FSHD: copy number variations on the theme of muscular dystrophy. *J Cell Biol* **191**: 1049–1060.
4. Lemmers, RJ, van der Vliet, PJ, Klooster, R, Sacconi, S, Camaño, P, Dauwerse, JG *et al.* (2010). A unifying genetic model for facioscapulohumeral muscular dystrophy. *Science* **329**: 1650–1653.
5. Gabellini, D, D'Antona, G, Moggio, M, Prelle, A, Zecca, C, Adami, R *et al.* (2006). Facioscapulohumeral muscular dystrophy in mice overexpressing FRG1. *Nature* **439**: 973–977.
6. Grewal, PK, Todd, LC, van der Maarel, S, Frants, RR and Hewitt, JE (1998). FRG1, a gene in the FSH muscular dystrophy region on human chromosome 4q35, is highly conserved in vertebrates and invertebrates. *Gene* **216**: 13–19.
7. Hanel, ML, Sun, CY, Jones, TI, Long, SW, Zanotti, S, Milner, D *et al.* (2011). Facioscapulohumeral muscular dystrophy (FSHD) region gene 1 (FRG1) is a dynamic nuclear and sarcomeric protein. *Differentiation* **81**: 107–118.
8. Brais, B, Bouchard, JP, Xie, YG, Rochefort, DL, Chrétien, N, Tomé, FM *et al.* (1998). Short GCG expansions in the PABP2 gene cause oculopharyngeal muscular dystrophy. *Nat Genet* **18**: 164–167.
9. Nicole, S, Diaz, CC, Frugier, T and Melki, J (2002). Spinal muscular atrophy: recent advances and future prospects. *Muscle Nerve* **26**: 4–13.
10. van Koningsbruggen, S, Dirks, RW, Mommaas, AM, Onderwater, JJ, Deidda, G, Padberg, GW *et al.* (2004). FRG1P is localised in the nucleolus, Cajal bodies, and speckles. *J Med Genet* **41**: e46.
11. van Koningsbruggen, S, Straasheijm, KR, Sterrenburg, E, de Graaf, N, Dauwerse, HG, Frants, RR *et al.* (2007). FRG1P-mediated aggregation of proteins involved in pre-mRNA processing. *Chromosoma* **116**: 53–64.
12. Reed, P, Porter, NC, Strong, J, Pumplin, DW, Corse, AM, Luther, PW *et al.* (2006). Sarcolemmal reorganization in facioscapulohumeral muscular dystrophy. *Ann Neurol* **59**: 289–297.
13. McNally, EM and Pytel, P (2007). Muscle diseases: the muscular dystrophies. *Annu Rev Pathol* **2**: 87–109.
14. Selcen, D (2008). Myofibrillar myopathies. *Curr Opin Neurol* **21**: 585–589.
15. Selcen, D and Carpén, O (2008). The Z-disk diseases. *Adv Exp Med Biol* **642**: 116–130.
16. Hanel, ML, Wuebbles, RD and Jones, PL (2009). Muscular dystrophy candidate gene FRG1 is critical for muscle development. *Dev Dyn* **238**: 1502–1512.
17. Wuebbles, RD, Hanel, ML and Jones, PL (2009). FSHD region gene 1 (FRG1) is crucial for angiogenesis linking FRG1 to facioscapulohumeral muscular dystrophy-associated vasculopathy. *Dis Model Mech* **2**: 267–274.
18. Liu, Q, Jones, TI, Tang, VW, Brieher, WM and Jones, PL (2010). Facioscapulohumeral muscular dystrophy region gene-1 (FRG-1) is an actin-bundling protein associated with muscle-attachment sites. *J Cell Sci* **123**(Pt 7): 1116–1123.
19. Fire, A, Xu, S, Montgomery, MK, Kostas, SA, Driver, SE and Mello, CC (1998). Potent and specific genetic interference by double-stranded RNA in Caenorhabditis elegans. *Nature* **391**: 806–811.
20. Davidson, BL and McCray, PB Jr (2011). Current prospects for RNA interference-based therapies. *Nat Rev Genet* **12**: 329–340.
21. McCaffrey, AP, Nakai, H, Pandey, K, Huang, Z, Salazar, FH, Xu, H *et al.* (2003). Inhibition of hepatitis B virus in mice by RNA interference. *Nat Biotechnol* **21**: 639–644.
22. Xia, H, Mao, Q, Eliason, SL, Harper, SQ, Martins, IH, Orr, HT *et al.* (2004). RNAi suppresses polyglutamine-induced neurodegeneration in a model of spinocerebellar ataxia. *Nat Med* **10**: 816–820.
23. DiGiusto, DL, Krishnan, A, Li, L, Li, H, Li, S, Rao, A *et al.* (2010). RNA-based gene therapy for HIV with lentiviral vector-modified CD34(+) cells in patients undergoing transplantation for AIDS-related lymphoma. *Sci Transl Med* **2**: 36ra43.
24. Mingozzi, F and High, KA (2011). Therapeutic *in vivo* gene transfer for genetic disease using AAV: progress and challenges. *Nat Rev Genet* **12**: 341–355.
25. Bantel-Schaal, U, Delius, H, Schmidt, R and zur Hausen, H (1999). Human adeno-associated virus type 5 is only distantly related to other known primate helper-dependent parvoviruses. *J Virol* **73**: 939–947.
26. Rutledge, EA, Halbert, CL and Russell, DW (1998). Infectious clones and vectors derived from adeno-associated virus (AAV) serotypes other than AAV type 2. *J Virol* **72**: 309–319.
27. Gao, GP, Alvira, MR, Wang, L, Calcedo, R, Johnston, J and Wilson, JM (2002). Novel adeno-associated viruses from rhesus monkeys as vectors for human gene therapy. *Proc Natl Acad Sci USA* **99**: 11854–11859.
28. Gregorevic, P, Blankinship, MJ, Allen, JM, Crawford, RW, Meuse, L, Miller, DG *et al.* (2004). Systemic delivery of genes to striated muscles using adeno-associated viral vectors. *Nat Med* **10**: 828–834.
29. Odom, GL, Gregorevic, P, Allen, JM and Chamberlain, JS (2011). Gene therapy of mdx mice with large truncated dystrophins generated by recombination using rAAV6. *Mol Ther* **19**: 36–45.
30. Wang, Z, Kuhr, CS, Allen, JM, Blankinship, M, Gregorevic, P, Chamberlain, JS *et al.* (2007). Sustained AAV-mediated dystrophin expression in a canine model of Duchenne muscular dystrophy with a brief course of immunosuppression. *Mol Ther* **15**: 1160–1166.
31. Paul, CP, Good, PD, Winer, I and Engelke, DR (2002). Effective expression of small interfering RNA in human cells. *Nat Biotechnol* **20**: 505–508.
32. Grimm, D, Streetz, KL, Jopling, CL, Storm, TA, Pandey, K, Davis, CR *et al.* (2006). Fatality in mice due to oversaturation of cellular microRNA/short hairpin RNA pathways. *Nature* **441**: 537–541.
33. McBride, JL, Boudreau, RL, Harper, SQ, Staber, PD, Monteys, AM, Martins, I *et al.* (2008). Artificial miRNAs mitigate shRNA-mediated toxicity in the brain: implications for the therapeutic development of RNAi. *Proc Natl Acad Sci USA* **105**: 5868–5873.
34. Boudreau, RL, Martins, I and Davidson, BL (2009). Artificial microRNAs as siRNA shuttles: improved safety as compared to shRNAs *in vitro* and in vivo. *Mol Ther* **17**: 169–175.
35. Beer, S, Bellovin, DI, Lee, JS, Komatsubara, K, Wang, LS, Koh, H *et al.* (2010). Low-level shRNA cytotoxicity can contribute to MYC-induced hepatocellular carcinoma in adult mice. *Mol Ther* **18**: 161–170.
36. Chen, JF, Murchison, EP, Tang, R, Callis, TE, Tatsuguchi, M, Deng, Z *et al.* (2008). Targeted deletion of Dicer in the heart leads to dilated cardiomyopathy and heart failure. *Proc Natl Acad Sci USA* **105**: 2111–2116.
37. Gabriëls, J, Beckers, MC, Ding, H, De Vriese, A, Plaisance, S, van der Maarel, SM *et al.* (1999). Nucleotide sequence of the partially deleted D4Z4 locus in a patient with FSHD identifies a putative gene within each 3.3 kb element. *Gene* **236**: 25–32.
38. Dixit, M, Ansseau, E, Tassin, A, Winokur, S, Shi, R, Qian, H *et al.* (2007). DUX4, a candidate gene of facioscapulohumeral muscular dystrophy, encodes a transcriptional activator of PITX1. *Proc Natl Acad Sci USA* **104**: 18157–18162.
39. Snider L, Asawachaicharn A, Tyler AE, Geng LN, Petek LM, Maves L *et al.* (2009). RNA transcripts, miRNA-sized fragments and proteins produced from D4Z4 units: new candidates for the pathophysiology of facioscapulohumeral dystrophy. *Hum Mol Genet* **18**:2414-2430.
40. Snider L, Geng LN, Lemmers RJ, Kyba M, Ware CB, Nelson AM *et al.* (2010). Facioscapulohumeral dystrophy: incomplete suppression of a retrotransposed gene. *PLoS Genet* **6**:e1001181.
41. Kowaljow, V, Marcowycz, A, Ansseau, E, Conde, CB, Sauvage, S, Mattéotti, C *et al.* (2007). The DUX4 gene at the FSHD1A locus encodes a pro-apoptotic protein. *Neuromuscul Disord* **17**: 611–623.
42. Bosnakovski, D, Xu, Z, Gang, EJ, Galindo, CL, Liu, M, Simsek, T *et al.* (2008). An isogenetic myoblast expression screen identifies DUX4-mediated FSHD-associated molecular pathologies. *EMBO J* **27**: 2766–2779.
43. Wuebbles, RD, Long, SW, Hanel, ML and Jones, PL (2010). Testing the effects of FSHD candidate gene expression in vertebrate muscle development. *Int J Clin Exp Pathol* **3**: 386–400.
44. Wallace, LM, Garwick, SE, Mei, W, Belayew, A, Coppee, F, Ladner, KJ *et al.* (2011). DUX4, a candidate gene for facioscapulohumeral muscular dystrophy, causes p53-dependent myopathy in vivo. *Ann Neurol* **69**: 540–552.
45. Gabellini, D, Green, MR and Tupler, R (2002). Inappropriate gene activation in FSHD: a repressor complex binds a chromosomal repeat deleted in dystrophic muscle. *Cell* **110**: 339–348.
46. Paul, CP, Good, PD, Li, SX, Kleihauer, A, Rossi, JJ and Engelke, DR (2003). Localized expression of small RNA inhibitors in human cells. *Mol Ther* **7**: 237–247.
47. Allen, JM, Halbert, CL and Miller, AD (2000). Improved adeno-associated virus vector production with transfection of a single helper adenovirus gene, E4orf6. *Mol Ther* **1**: 88–95.
48. Hu, JH, Navas, P, Cao, H, Stamatoyannopoulos, G and Song, CZ (2007). Systematic RNAi studies on the role of Sp/KLF factors in globin gene expression and erythroid differentiation. *J Mol Biol* **366**: 1064–1073.
49. Blankinship, MJ, Gregorevic, P, Allen, JM, Harper, SQ, Harper, H, Halbert, CL *et al.* (2004). Efficient transduction of skeletal muscle using vectors based on adeno-associated virus serotype 6. *Mol Ther* **10**: 671–678.
50. Halbert, CL, Standaert, TA, Aitken, ML, Alexander, IE, Russell, DW and Miller, AD (1997). Transduction by adeno-associated virus vectors in the rabbit airway: efficiency, persistence, and readministration. *J Virol* **71**: 5932–5941.